A SIMPLE NUMERICAL MODEL FOR SUPERCRITICAL FLOW IN CHANNEL JUNCTIONS

A Thesis Submitted
in Partial Fulfilment of the Requirements
for the Degree of
MASTER OF TECHNOLOGY

by

BOVIN KUMAR

to the

Department of Civil Engineering
Indian Institute of Technology, Kanpur

CERTIFICATE

This is to certify that the present research work entitled A Simple Numerical Model for Supercritical flow in Channel Junctions *has been carried out by* Bovin Kumar *under our supervision and it has not been submitted elsewhere for a degree.*

K. Subramanya.

Dr.K. Subramanya

Professor

Dept. of Civil Engineering

Indian Institute of Technology

Kanpur

B.S murty

Dr.B.S. MURTY

Asistant Professor

Dept. of Civil Engineering

Indian Institute of Technology

Kanpur

APRIL 1996

ABSTRACT

To analyze the flow in a supercritical channel junction, two dimensional, depth averaged unsteady flow equations are solved by using false transient approach. An algebraic coordinate transformation is used to obtain a rectangular computational domain to simplify the numerical treatment of boundaries. Results of numerical experimentation on 22.5° and 45° junctions are compared with those obtained by using approximate method of Hager as well as with the available experimental data . Comparison of the present numerical results for large confluence angles indicate satisfactory prediction of the maximum depth of flow when the flow in the main channel is dominant. However, for small confluence angles the results are not very satisfactory due to the inherent assumptions of the shallow water equations. The present numerical simulation is able to adequately simulate the water surface contours at the confluence qualitatively.

ACKNOWLEDGEMENTS

I express my profound sense of gratitude to my teachers **Dr. B.S. Murty** and **Dr. K. Subramanya** for suggesting the problem of this thesis and their guidance throughout the work. It was a memorable and an enjoyable experience to work with them.

I am thankful to the staff of the Hydraulics and Water Resources section of Civil Engineering Department especially my teachers Dr. S. Surya Rao, Dr. T. Gangadhriah, Dr. Bithin Datta and Dr. S.Ramasheshan who enforced my foundations in Civil Engineering.

I would like to express my appreciation for the tireless help, innumerable comments and suggestions my friends have given me. My thanks to them are inexpressible. Particularly I would like to thank Sandeep Sharma, Anand Tewari, K.S.Grover and Shubha Kapil for their help and inspiration which made my stay at Kanpur more enjoyable.

I wish to express my gratitude to the Dept. of Science and Technology for the financial support.

Lastly the author is thankful the Xerox centre of Hall-5 for Photocopying.

- Bovin Kumar

TABLE OF CONTENTS

NOTATION

CN	Courant Number
g	acceleration due to gravity, cm/s^2
F_u	Froude number in the main channel
F_l	Froude number in the lateral channel
h_u	flow depth in the main channel, cm
h_l	flow depth in the lateral channel, cm
i	subscript for space node in ξ direction
j	subscript for space node in η direction
n	subscript for time level
S_{ox}	channel bottom slope in x-direction
S_{oy}	channel bottom slope in y-direction
S_{fx}	friction slope in x-direction
S_{fy}	friction slope in y-direction
t	time
u	flow velocity in x-direction
v	flow velocity in y-direction
V	magnitude of resultant velocity
x	space coordinate
y	space coordinate

Greek letters

α	confluence angle of lateral channel with main channel
α_x	angle between of channel and the x-direction
α_y	angle between of channel and the y-direction
β	angle of wave front
γ	coefficient used in the numerical scheme
θ	angle of streamlines in the shock
η	transformed space coordinate
ξ	transformed space coordinate
Δt	time interval
$\Delta\eta$	distance increment in η direction
$\Delta\xi$	distance increment in ξ direction

LIST OF FIGURES

Chapter 1

Introduction

Open channel flows,whether in natural channels or in man-made situations, is predominantly in subcritical mode. Supercritical flows are rather rare and are also more complicated to analyze than their subcritical counterparts. Not surprisingly, the knowledge base relating to these supercritical flow situations is relatively less.

Channel junctions are necessary component of a channel network. Junction of flow of two or more supercritical flows are sometimes encountered in mountaneous stream networks and in road drainage works. The flow situations in the channel junctions may be any of the following kinds The flows in the lateral channel and main channel before the junction are supercritical but after the junction it becomes subcritical or flow in any of the channels is supercritical and after the junctions it becomes subcritical or it may be that it is supercritical in both the channels and remains so after the junction. Here such type of junctions are being studied where the flows are supercritical in main channel, lateral channel and it remains

supercritical after the junction. Here onwards this type of junctions will be referred to as SC junctions for the rest of the report. Supercritical flow in a combining channel junction is accompanied by standing waves which persists for long distances downstream of the channel junction. The side walls for such a junction have to be considerably higher than normal because the maximum height of the free surface may be 10 to 20 times as large as the depth of incoming flow (Behlke and Pritchett 1966, Greated 1968). A hydraulic jump may form for certain combinations of junction configuration and the inflow conditions. This leads to the problem in closed channels such as tunnel spillways due to pulsation, air entrainment and transition to pressurized flow (Hager 1989)

Analysis of supercritical flow is more complicated than the subcritical flow because of the presence of cross waves. Bowers (1950) was probably the first person to study SC junctions. Schnitter et al. (1955) conducted experimental studies in the channel junctions with small confluence angles and found that a significant cross wave pattern is developed when the Froude numbers in the two upstream branches are not equal. Behlke and Pritchett (1966) and Greated (1968) presented a analytical approach for determining wave angles in simple junctions and identified wall pile up zones. Gerodetti (1978) conducted experiments in junctions of semi-circular channels and steep bottom slopes. Hager (1989) used both analytical and experimental approaches to analyze the main flow features in simple SC junctions. He

considered rectangular cross sections and junction angles of 22.5° and 45° .

Characteristics of supercritical flow can also be obtained by solving the two dimensional steady flow equations numerically. In spite of the significant advances and the refinement of computations of open channel flows, supercritical flow still defy reliable analysis. The basic equations are hyperbolic partial differential equations and such method of charateristic may be used to solve these equations. Yet for the two dimensional cases the method is too complicated. Bagge and Herbich (1967), Herbich and Walsh (1972), Villagas (1976) and Dakshinamoorthy (1973, 1977) used this method for analyzing steady state supercritical flows in channel transitions. The analogy between gas dynamics and shallow water flow has prompted many researchers to borrow techniques developed in the former area and apply them to supercritical flows in open channels. There are two types of techniques to compute flow fields with shocks ; the *shock fitting* and *shock capturing* techniques. Shock fitting methods treat shocks as discontinuities and explicitly compute their motion and strength, while shock capturing techniques do not give any special treatments to the shocks and their motion and strength is predicted as the part of the solution.

Jimenez (1987) and Jimenez and Chaudhary (1988) used shock capturing technique to simulate supercritical flow in transitions. Shock capturing techniques are capable of solving steady supercritical flow equations and marching technique may be used to simulate the oblique jumps or shocks. It fails for the case when the flow

anywhere in the channel becomes subcritical as the governing equations become elliptic. Using unsteady flow model to obtain steady state flow solution by solving false transient approach mixed subcritical and supercritical flow may be simulated. Such techniques have been applied in the past to simulate supercritical flows in channel transitions, among others, by Ligget and Vasudev (1965) Pandolfi (1982), and Jimenez and Chaudhary (1988). Bhallamudi and Chaudhary (1992) used two dimensional unsteady flow equations and the false transient approach to solve the same problem. This model can also simulate mixed sub and supercritical flows satisfactorily.

In the present study, a two dimensional numerical model based on the false transient approach is presented for computation of supercritical flows in simple channel junctions. A simple algebraic technique is used to convert the physical domain of the channel junction into a convenient computational domain. This makes the application of shock capturing finite difference methods easier. The computed results are compared with the experimental and analytical results of Hager (1989) to demonstrate the validity of the model. Brief introduction of analytical approach is given in the next section .

1.1 Analytical approach for maximum depth in the channel junction

The following model is based essentially on the analytical approach of Hager (1989). Fig(1.1) shows an idealized channel junction which is considered to be divided into three zones. these are

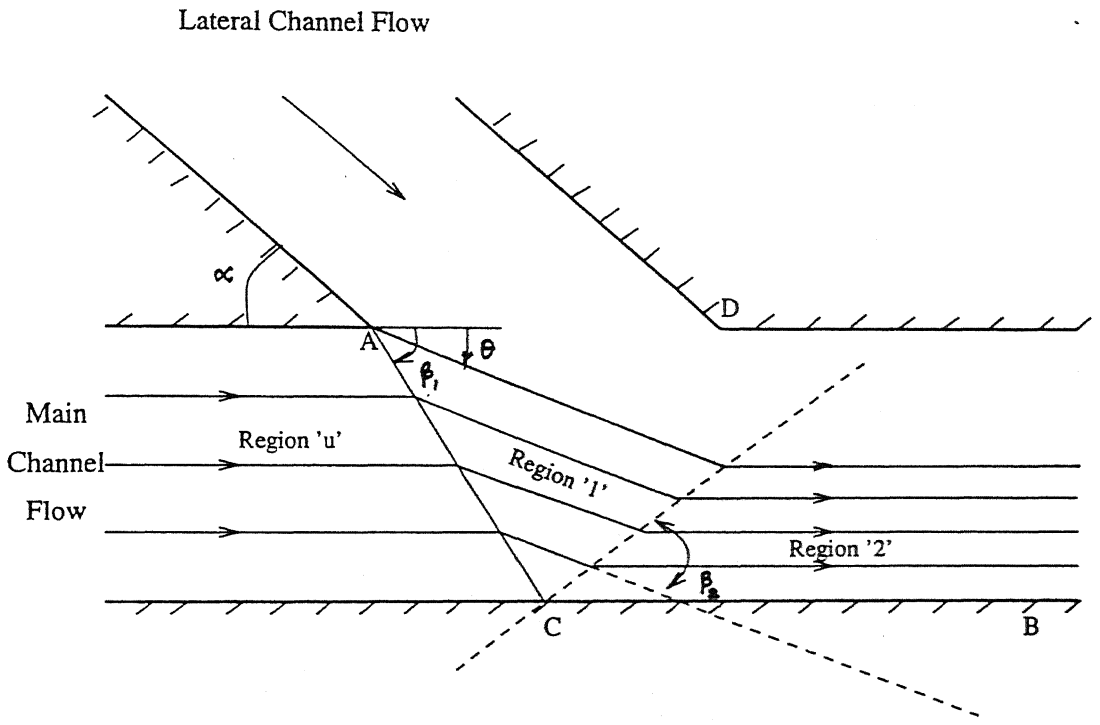

Fig(1.1): Supercritical flow in a channel junction

1. Upstream zone (*suffix u*)

2. Zone between angle θ and β_1 (*suffix 1*)

3. Zone between wall and wave front with the angle β_2 (*suffix 2*)

Fig(1.1) also shows the streamline pattern of the main flow. The depth of flow increases across the jumps and reaches a maximum in the *zone 2*. This maximum flow depth and can be estimate as

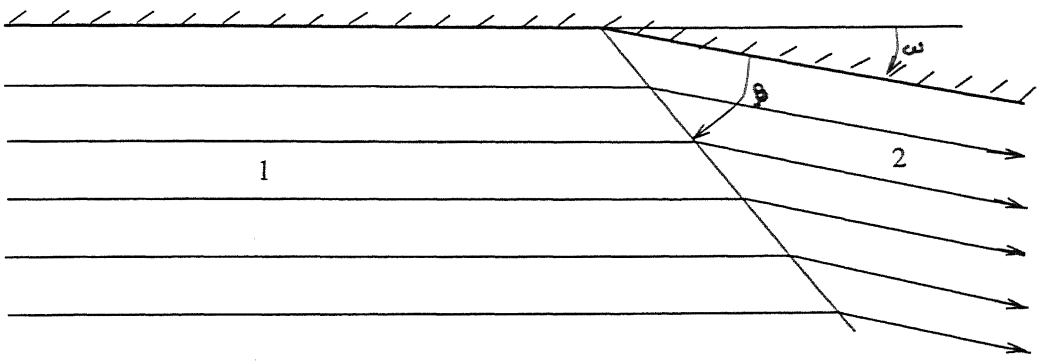

Fig(1.2): Supercritical flow past a wall deflection

follows. Consider a supercritical flow past a wall deflection as shown in the Fig(1.2), the following relationships are used to determine h_2, F_2, β_2 if h_1, F_1, ω are given (Subramanya.1995)

$$y = \frac{h_2}{h_1} = \frac{1}{2}\left[\sqrt{1 + 8F_1^2 + \sin^2\beta} - 1\right] \tag{1.1}$$

$$\frac{h_2}{h_1} = \frac{\tan\beta}{\tan(\beta - \omega)} \tag{1.2}$$

$$F_2^2 = \frac{1}{y}\left[F_1^2 - \frac{1}{2y}(y-1)(y+1)^2\right] \tag{1.3}$$

As the determination of h_2, F_2 and β is implicit in the above system of equations, Hager and Bretz (1987) derived the following explicit approximate equation from

the above equations.

$$\frac{h_2}{h_1} = \sqrt{2}F_1 \sin\beta - \frac{1}{2} \tag{1.4}$$

$$\beta = \omega + \frac{3}{2\sqrt{2}F_1} \tag{1.5}$$

$$F_2^2 = \frac{F_1^2 \cos^2\beta}{\sqrt{2}\sin\beta\left(1 - \frac{1}{2f_1}\right)} \tag{1.6}$$

where

$$f_1 = \sqrt{2}F_1\beta \tag{1.7}$$

Applying above equations for *region u* and *region 1* to get y_1, F_1, β_1 and then for *region 1* to *region 2* to get y_2, F_2, β_2, the depth h_2 can be computed.

To calculate θ Greated (1985) assumed uniform velocity and hydrostatic distribution and derived the following relationship.

$$1 - y^2 = 2y^2F_u^2\sin^2\theta - 2F_l^2\sin^2(\alpha - \theta) \tag{1.8}$$

Hager (1989) further simplified Eqn.(1.8) and expressed θ as

$$\frac{\theta}{\alpha} = \left[1 + \frac{V_u}{V_l}\sqrt{\frac{h_u}{h_l}}\right]^{-1} \tag{1.9}$$

where $y = \frac{h_u}{h_l}$

All the analysis by Hager is valid only if the confluence angle is $\leq 45^o$

Chapter 2

Governing Equations

Open channel flows are described by three conservation laws viz. laws of conservation of mass, momentum and energy. If there are no discontinuities like jump or bore the momentum coefficient β, and velocity coefficient α, are same and hence the momentum equation and energy equation are identical (Cunje et al,1980). For a supercritical flow in a channel junction an oblique hydraulic jump takes place and hence the momentum equation is appropriate. Though shallow water equations are not exactly applicable to such a case yet more general equations describing flows in open channel like Bousinesq type equations (which include vertical acceleration effect) are not simple even for one dimensional flows. Therefore, the shallow water equations are used in this study to analyze flows in SC junction.

In this chapter the shallow water equations, alongwith their assumptions and limitations are presented. This is followed by the co-ordinate transformation procedure for transforming the physical plane into a rectangular plane.

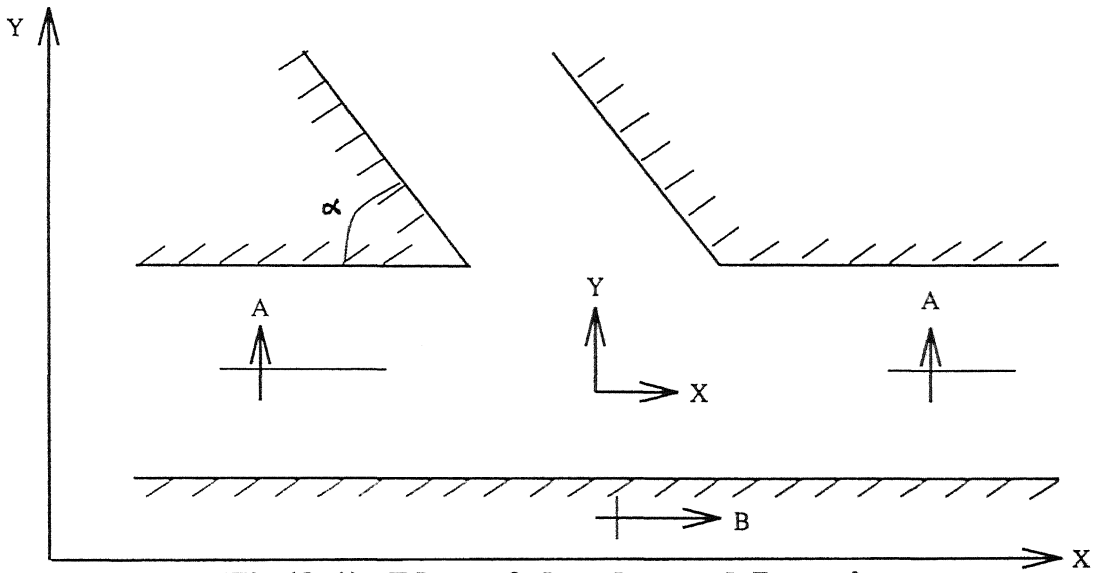

Fig(2.1): Plan of the channel Junction

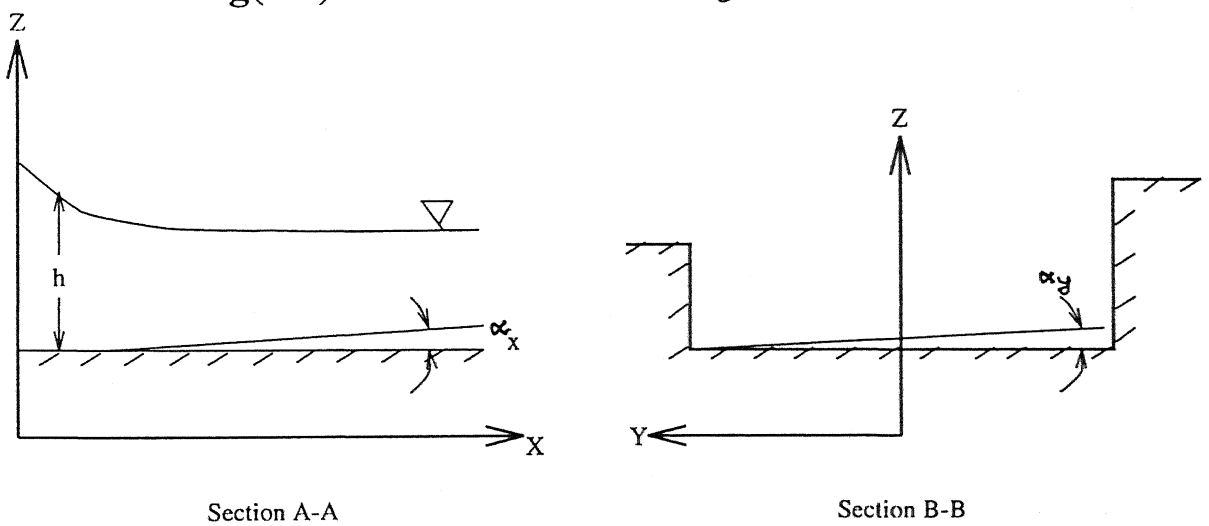

Section A-A

Section B-B

Fig(2.2): Sections of Channel Junction

2.1 Shallow Water Equations

Although in reality the flow in a SC junction is three-dimensional, for the purpose of analysis a two-dimensional approximation is adopted. Towards this vertically averaged quantities are used which simplifies the analysis and yields the results to reasonable accuracy.

The governing equations are derived by depth averaging the 3-dimensional equations over the flow depth. The equations in cartesian system are written as

$$U_t + F_x + G_y + S = 0 \tag{2.1}$$

where

$$U = \begin{pmatrix} h \\ hu \\ hv \end{pmatrix}$$

$$F = \begin{pmatrix} uh \\ u^2h + \frac{1}{2}gh^2 \\ uvh \end{pmatrix}$$

$$G = \begin{pmatrix} vh \\ uvh \\ v^2h + \frac{1}{2}gh^2 \end{pmatrix}$$

$$S = \begin{pmatrix} 0 \\ -gh(S_{ox} - S_{fx}) \\ -gh(S_{oy} - S_{fy}) \end{pmatrix}$$

subscripts t, x and y in Eqn 2.1 represents the partial derivative with respect to time, longitudinal direction and lateral direction respectively.

In the above equation,

t = time

u = velocity along longitudinal direction

v = velocity along lateral direction

h = water depth measured vertically

g = acceleration due to gravity

S_{ox} = channel slope along longitudinal direction

S_{oy} = channel slope along lateral direction

S_{fx} = friction slope along longitudinal direction

S_{fy} = friction slope along lateral direction

The bottom slopes are estimated as:

$$S_{ox} = \sin \alpha_x \tag{2.2}$$

$$S_{oy} = \sin \alpha_y \tag{2.3}$$

α_x,α_y are the angles between the bottom of the channel and the longitudinal and lateral direction respectively as shown in Fig(2.1) and Fig(2.2).

Friction slopes may be estimated using Manning's or Chezy's equation. For example :

$$S_{fx} = \frac{u\sqrt{u^2+v^2}}{C^2 h} \tag{2.4}$$

$$S_{fy} = \frac{v\sqrt{u^2+v^2}}{C^2 h} \tag{2.5}$$

where C = Chezy's coefficient

2.2 Assumptions:

Shallow water equations are based on the following assumptions :

1. The pressure distribution in the vertical direction is assumed to be hydrostatic i.e. assuming the acceleration in the vertical direction negligible.

2. Depth averaged values are used in two-dimensional modelling.

3. Fluid is assumed to be incompressible and the density is same throughout.

4. Velocity distribution is uniform along the depth.

5. The channel bottom is rigid and the slope is negligible.

6. Only shear stresses due to horizontal velocity components are significant, other viscous effects are neglected.

7. Frictional resistance is approximated by the Chezy's equation or Manning's equation.

The chief assumptions viz. 1 and 2 are discussed in the following paragraphs:

2.2.1 Hydrostatic Pressure distribution:

The assumption of hydrostatic distribution is correct if the streamlines are parallel and straight. As long as high curvatures are not present the the pressure distribution is almost hydrostatic. Ligget (1975) had shown that the assumption is valid as long as a *shallowness parameter* h_0/l_0 (h_0 is water depth and l_0 is characteristic length) is small. Later Jimenez (1987) concluded that the shallow water theory reasonably represents the supercritical flow if depth to width ratio is of the order of 0.1 and Froude number is not close to unity. The error is of the order of 20% if the depth to width ratio is increased to 0.2. This error is manifested in the wavelength of the resulting wave pattern. The hydrostatic assumption is not valid in the vicinity of the shock and some flow details are lost at the shock location. However the overall results are adequate for engineering purposes (Cunge 1975).

2.2.2 Turbulent effects and Depth averaging:

The depth integration of the three-dimensional equations of motion produce higher order terms known as effective stresses which are not included in the Eqn(2.1). Effective stresses constitute laminar viscous stresses, turbulent stresses and stresses due

to depth averaging of advective terms. Laminar viscous stresses may be neglected but the other two are important. Consideration of turbulent stresses require the use of turbulence closure model which expresses stresses as a function ϵ of the main flow variables. Rastogi and Rodi (1978), Puri and Kao (1984) and Leschziner and Rodi (1979) used $K - \epsilon$ models for describing turbulence. Vreugdenhil and Wijbenga (1982) used constant eddy viscosity concept. However, the above closure models are tested only for subcritical flows and no information is available for supercritical flows. Without considering turbulent terms the side wall boundary layer effects are omitted. Ippen and Harleman (1950) analyzed the case of oblique jump and concluded that reduction of velocity across the boundary layer reduces the vertical acceleration at the point of wall deflection. This makes the shock front steeper than in the case when the boundary layer in not included.

Ippen and Harleman (1950) studied the effect of non-uniform velocity distribution also. They concluded that the effect of velocity distribution may be considered negligible.The measurement of velocity across the depth on the front and back side of the jump indicated that the momentum correction factor ranged from 1.007 at $F_r = 6.3$ to 1.015 at $F_r = 2.0$. It should be noted that though the effect of magnitude variation of velocity may not be significant yet the variation of the direction of resultant velocity across the depth is significant. Especially in the channel junction as found by Hager (1989) the velocity vectors at different depths for supercritical

flow are not same. Velocity is almost parallel to the side wall near the channel bottom and it is pointing towards the wall near the surface. Eqn(2.1) can not simulate this effect and the numerical results will be in error.

2.3 Coordinate Transformation:

In this study, a finite-difference method is used to solve Eqn(2.1). Physical boundary as well as the finite difference grid in cartesian coordinate system for a channel junction are shown in Fig(2.3).

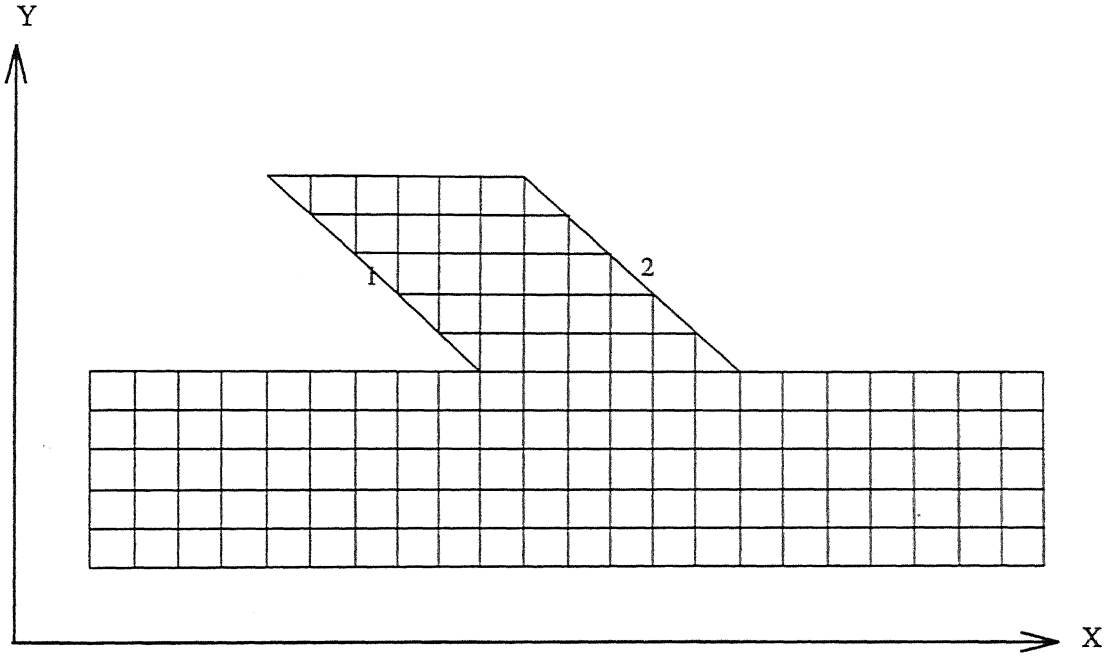

Fig(2.3): Finte difference grid superposed on channel

We notice that it becomes necessary to represent physical boundary in angular portion in a stair step fashion. It leaves sharp corners (marked 1 on left side and 2 on

right side) which introduce numerical disturbances which spread quickly to entire mesh. This may result into numerical instability (Roache 1972) particularly for supercritical flows which are hyperbolic in nature. An alternate method of arranging the grid could be as in Fig(2.4)

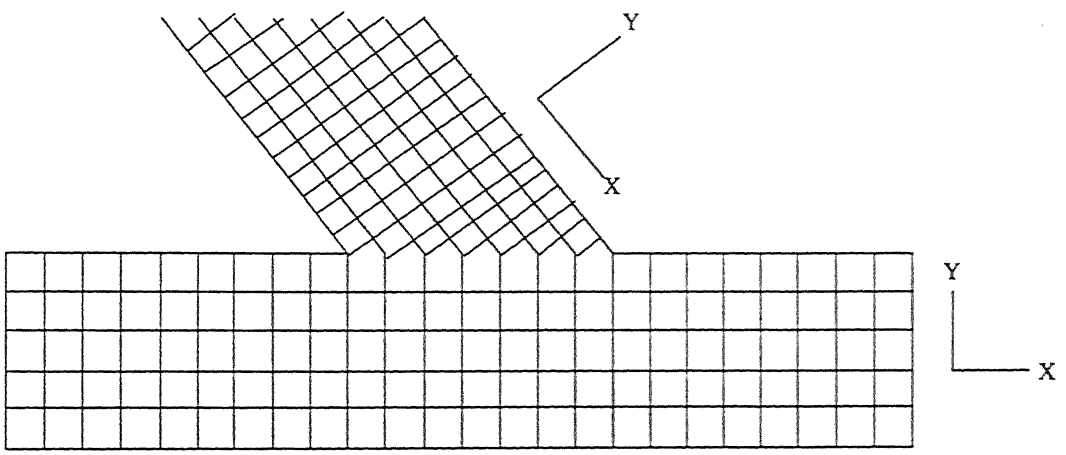

Fig(2.4): A second arrangement of grid

This again leaves wedges at junctions of two channels and also require different coordinate directions for straight and angular channels. These problems can be avoided by using a coordinate system such that the coordinate axes coincide with the boundaries (Anderson et. al. 1984). Use of a simple algebraic coordinate transformation suffices in the present case Fig(2.5a). The following transformation of independent variables convert the original physical plane Fig(2.5a) into a rectangular

computational plane Fig(2.5b).

$$\xi = x + y \cot \alpha \tag{2.6}$$

$$\eta = \frac{y}{\sin \alpha} \tag{2.7}$$

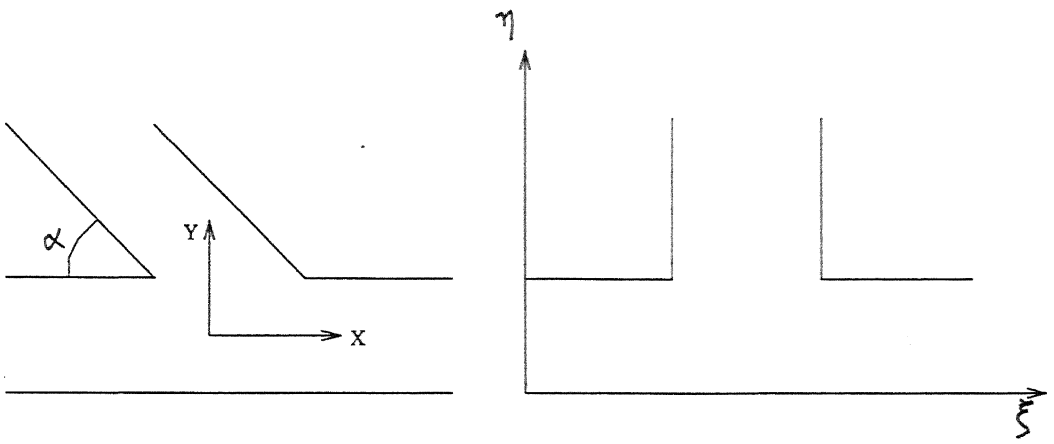

Fig(2.5a): Physical Plane **Fig(2.5b): Computational Plane**

With this, coordinate axes coincide with physical boundaries (see Fig(2.5c))

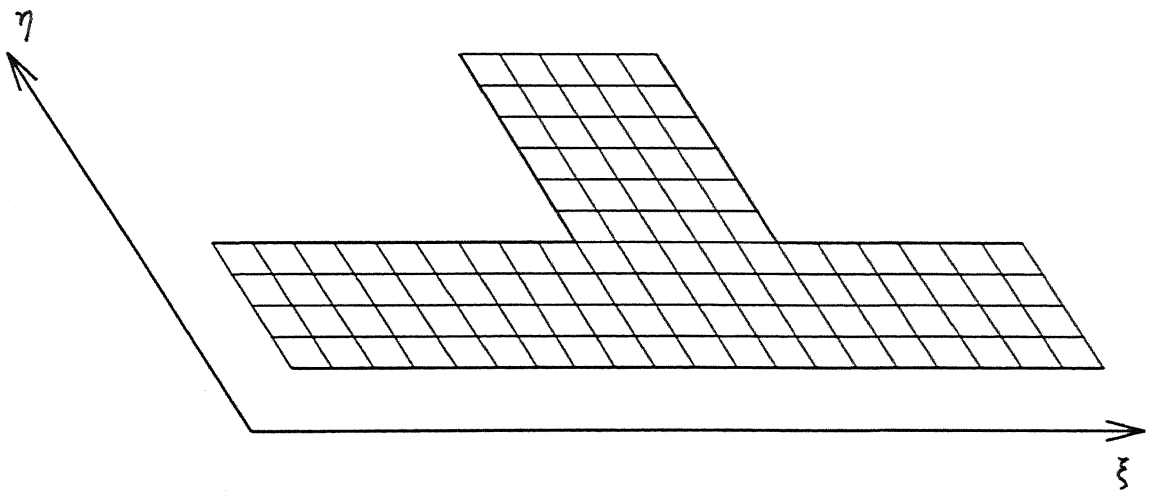

Fig(2.5c): Final Grid

The governing equations must be expressed in terms of the new independent variables for their application. This is done by applying the chain rule of partial differentiation as follows:

$$\frac{\partial}{\partial x} = \xi_x \frac{\partial}{\partial \xi} + \eta_x \frac{\partial}{\partial \eta} \tag{2.8}$$

$$\frac{\partial}{\partial y} = \xi_y \frac{\partial}{\partial \xi} + \eta_y \frac{\partial}{\partial \eta} \tag{2.9}$$

Subscripts denote partial derivatives. Eqn(2.6) and Eqn(2.7) give

$$\xi_x = 1; \qquad \eta_x = 0 \tag{2.10}$$

$$\xi_y = \cot\alpha; \qquad \eta_y = \frac{1}{\sin\alpha} \tag{2.11}$$

$$\frac{\partial}{\partial x} = \frac{\partial}{\partial \xi}; \frac{\partial}{\partial y} = \cot\alpha \frac{\partial}{\partial \xi} + \left(\frac{1}{\sin\alpha}\right) \frac{\partial}{\partial \eta} \tag{2.12}$$

Applying the aforesaid transformations to the Eqn(2.1) and subsequently rearranging them yields the following equations.

$$\overline{U}_t + \overline{F}_\xi + \overline{G}_\eta + \overline{S} = 0 \tag{2.13}$$

where

$$\overline{U} = \begin{pmatrix} h \\ hu \\ hv \end{pmatrix}$$

$$\overline{F} = \begin{pmatrix} uh + hv\cot\alpha \\ u^2h + \frac{1}{2}gh^2 + huv\cot\alpha \\ uvh + (hv^2 + \frac{1}{2}gh^2)\cot\alpha \end{pmatrix}$$

$$\overline{G} = \begin{pmatrix} vh/\sin\alpha \\ uvh/\sin\alpha \\ (v^2h + \frac{1}{2}gh^2)/\sin\alpha \end{pmatrix}$$

$$\overline{S} = \begin{pmatrix} 0 \\ -gh(S_{ox} - S_{fx}) \\ -gh(S_{oy} - S_{fy}) \end{pmatrix}$$

Eqn(2.13) is solved in this study using a finite-difference method. The details of the numerical scheme are presented in the following chapter.

Chapter 3

Numerical scheme

3.1 Introduction

The shallow water equations are hyperbolic partial differential equations. Analytical solution for these equations is possible only for very simplified cases. Therefore one has to opt for the numerical techniques for solving these equations. Among numerical schemes either it may be finite-difference technique or finite-element technique. These days finite volume methods are also becoming popular to solve such type of problems yet these methods are used to solve the equations in the integral form . In this study a finite difference method is used to solve the Eqn(2.13) for a channel junction. It is required that we get the steady state conditions in the junction. For that we assume some initial conditions as constant depth and velocity throughout the main channel and constant velocity and constant depth in the lateral channel. The boundary conditions are set equal to the steady state conditions. Then the two dimensional unsteady flow equations are solved for sufficient length of time until

variation of flow conditions is negligible and the conditions have converged to steady state values for the given boundary conditions . The Method of characteristics with shock capturing procedure (for two dimensionals cases) take high computational effort. As such it is advantageous to use shock capturing techniques rather than the method of characteristics. In these methods the following three points should be noted.:

1. The governing partial differential equations should be in conservation form because Eqn(2.1) expresses the law of conservation of mass and momentum, and these quantities are conserved through the jump.

2. The numerical scheme should be conservative i.e it should maintain the discretised version of conservation laws throughout the computational region.

3. The numerical scheme should be dissipative in nature so that it could represent the energy loss associated with the hydraulic shocks. The dissipation should be in such a way that it is small in gradual variation, but comparitively large near the discontinuities (Abbot 1975). First order schemes are dissipative in nature but the higher order schemes which do not have this mechanism produce spurious oscillations near the discontinuities. These spurious oscillations are originated because the conservative variables being differentiated across the discontinuities (shocks) may have discontinuous derivatives. To reduce these oscillations some researchers generally go for *artificial viscosity* and align one

of the coordinate axis in the direction of shock.

Artificial viscosity which is added in order to reduce oscillations acts otherway and it adds to the dissipation. As the first order schemes are highly dissipative and the second order schemes are having dispersive error as well as these schemes produce spurious oscillations. Therefore need was felt to develop a scheme which is not highly dissipative as well as does not produce spurious oscillation. For that researchers thought of going for total variation diminishing (TVD) schemes. Although the approximate Riemann solver based on the flux difference splitting of Roe and a flux-vector splitting of Van-Leer approaches are very accurate yet the methods require significant computational and programming time because of the field by field

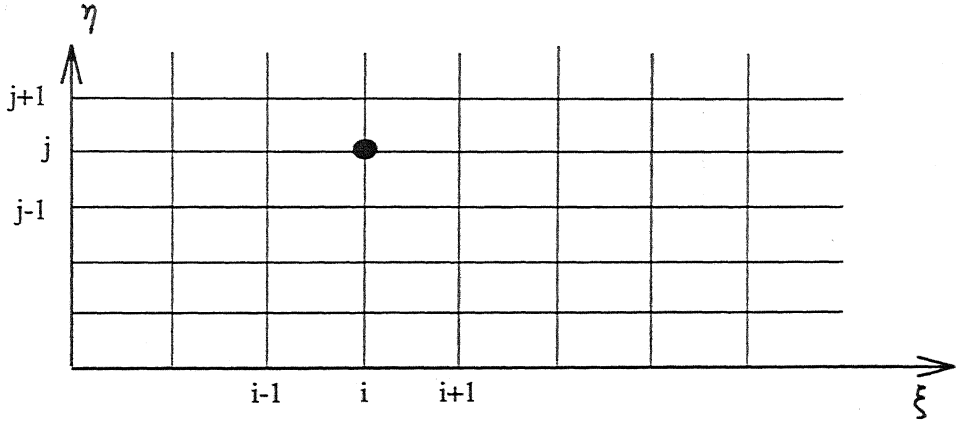

Fig(3.1): Finite Difference Grid

decomposition. In the present study non oscillatory numerical scheme based upon the Lax -Friedrich's solver proposed by Marinko Nujic (1995) has been used. The scheme has an advantage of its simplicity and ease of implimentation. Further it the

scheme treats the dispersion equation or turbulence model equations in the same way because Lax - Friedrichs solver does not depend on the structure of the hyperbolic system like the approximate solver which use field by field decomposition. The finite difference grid used in the scheme is shown in Fig (3.1). Here $\Delta\xi$ and $\Delta\eta$ are the mesh steps in ξ and η directions and i and j subscripts are used in the following section to indicate the position along ξ and η directions respectively.

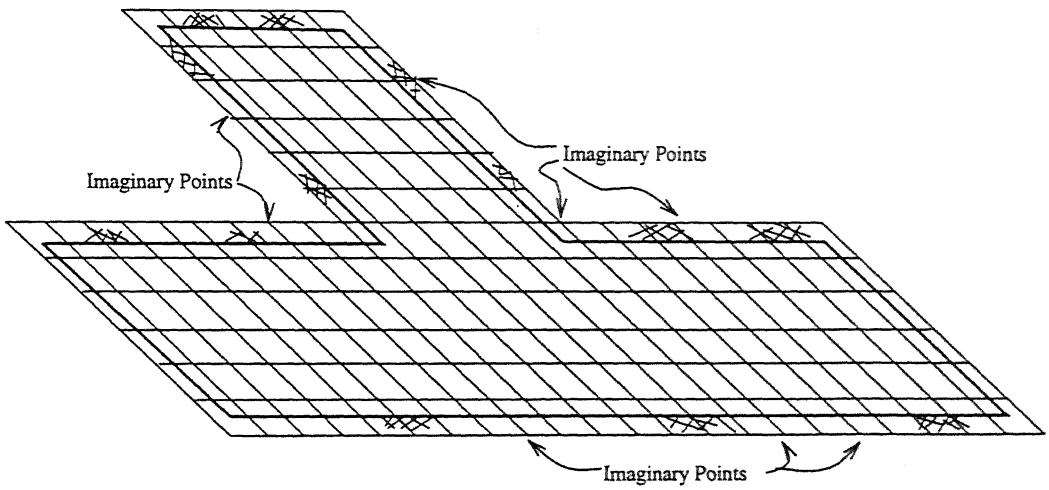

Fig(3.2): Finite Difference Grid with imaginary points

The dependent variables are known at any time level either as initial conditions or through computations for the previous step. The values of the variables at time $t + \Delta t$ are determined using the finite difference technique as detailed in the next section.

3.2 Nujic's Scheme

The scheme presented by Nujic to solve the hyperbolic partial differential equation is second order accurate. Only the brief introduction of the scheme for this problem is being described here. For the equation (2.1) the variable u may be approximated at $t + \Delta t$ (i.e. $n + 1^{th}$ time level) when everything is known at time t (i.e. n^{th} time level) in the following predictor and corrector form.

$$u^{\star}_{i,j} = u^{n}_{i,j} - \frac{\Delta t}{\Delta x}\left(f^{n}_{i+\frac{1}{2},j} - f^{n}_{i-\frac{1}{2},j}\right) - \frac{\Delta t}{\Delta y}\left(g^{n}_{i,j+\frac{1}{2}} - g^{n}_{i,j-\frac{1}{2}}\right) - S^{n}_{i,j}\Delta t \tag{3.1}$$

$$u^{n+1}_{i,j} = 0.5\left[u^{n}_{i,j} + u^{\star}_{i,j} - \frac{\Delta t}{\Delta x}\left(f^{\star}_{i+\frac{1}{2},j} - f^{\star}_{i-\frac{1}{2},j}\right) - \frac{\Delta t}{\Delta y}\left(g^{\star}_{i,j+\frac{1}{2}} - g^{\star}_{i,j-\frac{1}{2}}\right) - S^{\star}_{i,j}\Delta t\right] \tag{3.2}$$

where f and g are fluxes in ξ and η direction and $f_{i+\frac{1}{2},j}$ and $g_{i,j+\frac{1}{2}}$ are defined as

$$f_{i+\frac{1}{2},j} = 0.5\left[f^{R}_{i,j} + f^{L}_{i,j} - \gamma\left(u^{R}_{i,j} - u^{L}_{i,j}\right)\right] \tag{3.3}$$

$$g_{i,j+\frac{1}{2}} = 0.5\left[g^{B}_{i,j} + g^{T}_{i,j} - \gamma\left(u^{B}_{i,j} - u^{T}_{i,j}\right)\right] \tag{3.4}$$

in which

$$u^{L}_{i,j} = u_{i,j} + 0.5\delta u_{i,j} \tag{3.5}$$

$$u^{R}_{i,j} = u_{i+1,j} + 0.5\delta u_{i+1,j} \tag{3.6}$$

where

$$\delta u_{i,j} = minmod\left(u_{i+1,j} - u_{i,j}, u_{i,j} - u_{i-1,j}\right) \tag{3.7}$$

$$\delta u_{i+1,j} = minmod\left(u_{i+1,j} - u_{i,j}, u_{i+2,j} - u_{i+1,j}\right) \tag{3.8}$$

and

$$u_{i,j}^{T} = u_{i,j} + 0.5\delta u_{i,j} \tag{3.9}$$

$$u_{i,j}^{B} = u_{i,j+1} + 0.5\delta u_{i,j+1} \tag{3.10}$$

where the quantities $\delta u_{i,j}$ and $\delta u_{i,j+1}$ are

$$\delta u_{i,j} = minmod\left(u_{i,j+1} - u_{i,j}, u_{i,j} - u_{i,j-1}\right) \tag{3.11}$$

$$\delta u_{i,j+1} = minmod\left(u_{i,j+1} - u_{i,j}, u_{i,j+2} - u_{i,j+1}\right) \tag{3.12}$$

and the function minmod is defined as

$$minmod(a,b) = \begin{cases} a \; if \; |a| < |b| \; and \; ab > 0 \\ b \; if \; |b| < |a| \; and \; ab > 0 \\ 0 \; if \; ab \leq 0 \end{cases}$$

$f_{i,j}^{R}$, $f_{i,j}^{L}$, $g_{i,j}^{B}$ and $g_{i,j}^{T}$ can be calculated in the same way.

The above procedure can be used for the interior nodes. Boundary conditions have to be applied at the boundary nodes.

3.3 Initial and Boundary conditions :

In the false transient approach any initial conditions such as constant velocity and constant depth equal to the boundary value may be assumed for all nodes. The determination of u, v, h during the unsteady computations involve the application of boundary conditions. Hyperbolic equations are sensitive to the boundary conditions because errors introduced at the boundaries propagate and reflect throughout the

grid and in many cases the instability may result (Anderson et. al. 1984). There are two type of following boundaries in the present study . These are flow boundaries and solid side wall boundaries.

3.3.1 Flow Boundaries

Mathematical basis for the specification of the boundaries in the shallow water wave applications have been discussed by Stokes (1957) ,Abbott (1979) and Cunje et. al. Since the flow is two dimensional supercritical flow three boundary conditions are to be specified at the inflow boundaries and none at the outflow boundary.

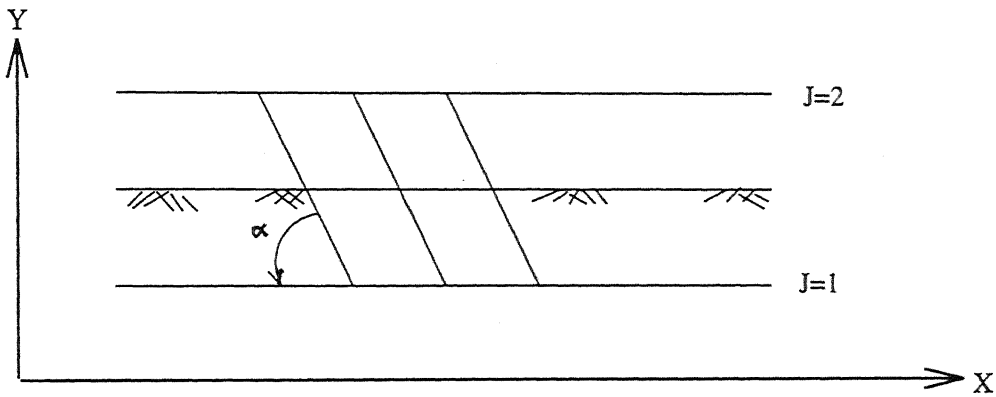

Fig(3.3): Illustration of Boundary Grid

In the present study u, v, h are specified at the inflow boundaries of the main channel and lateral channel and the downstream nodes these quantities are obtained by extrapolation from the value at the interior nodes already calculated . Since the flow is supercritical their extrapolation affects only a few points at the downstream

end and the disturbance can not travel upstream .

3.3.2 Solid Side wall boundary

Since all the stresses other than the bottom stresses are neglected the slip condition is the proper boundary condition for the solid boundaries . The basic requirement is no flow normal to the boundaries, which is expressed as

$$\tan\delta = \frac{v}{u} \tag{3.13}$$

where δ is the angle between the wall and the axis. For the side walls of the main channel reflection procedure has been adopted because $v = 0$ normal to the side walls as the walls are aligned along the x-axis. Because of the coordinate transformation the reflection procedure is slightly modified. The mathematical representations of reflection procedure in cartesian coordinate system is as below:

$$\frac{\partial h}{\partial y_{wall}} = 0 \tag{3.14}$$

$$\frac{\partial u}{\partial y_{wall}} = 0 \tag{3.15}$$

$$\frac{\partial v}{\partial y_{wall}} = \frac{2v_{wall}}{\Delta y} \tag{3.16}$$

Substituting Eqn(2.6) to Eqn(2.12) in Eqn(3.14) to Eqn(3.16) results in the following equations

$$\cos\alpha\frac{\partial h}{\partial \xi} + \frac{\partial h}{\partial \eta} = 0 \tag{3.17}$$

$$\cos\alpha\frac{\partial u}{\partial \xi} + \frac{\partial u}{\partial \eta} = 0 \tag{3.18}$$

$$\cos\alpha\frac{\partial v}{\partial \xi}+\frac{\partial v}{\partial \eta}=\frac{2v}{\Delta\eta} \tag{3.19}$$

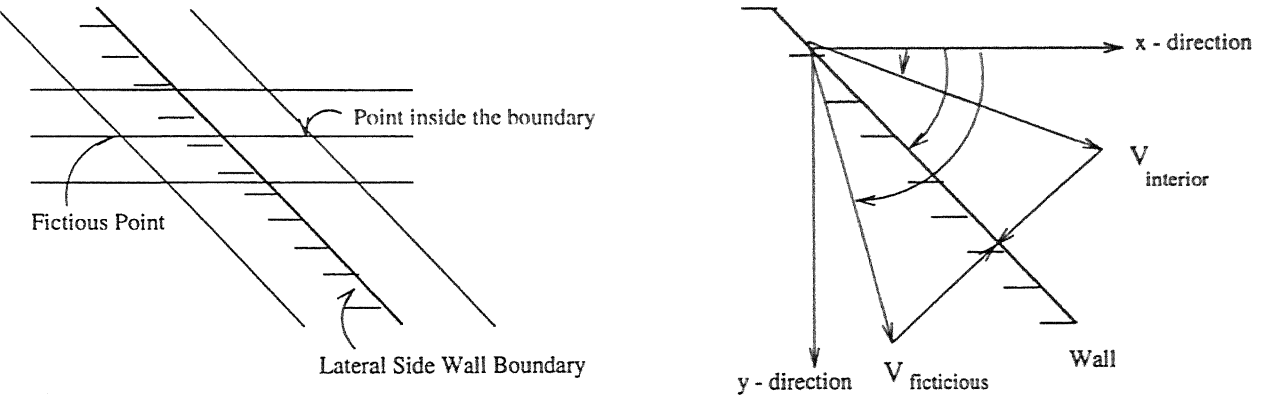

Fig(3.4) : Illustration of boundary Conditions at the wall in lateral channel.

Finite difference approximation of equations 3.12 to 3.14 for the solid wall shown in Fig(3.3) gives the following explicit equations for the determining h, u and v at any node, $(i,1)$

$$h_{i,1}=h_{i,2}+\frac{\Delta\eta}{\Delta\xi}\left(h_{i+1,2}-h_{i,2}\right)\cos\alpha \tag{3.20}$$

$$u_{i,1}=u_{i,2}+\frac{\Delta\eta}{\Delta\xi}\left(u_{i+1,2}-u_{i,2}\right)\cos\alpha \tag{3.21}$$

$$v_{i,1}=-v_{i,2}+\frac{\Delta\eta}{\Delta\xi}\left(v_{i+1,2}-v_{i,2}\right)\cos\alpha \tag{3.22}$$

As u, v ,h and fluxes are required at wall which is at midway of the nodal point as shown in the Fig(3.3).so the depth and velocity is the average of the depth at the ficticious points and the nodes adjacent to walls and velocity $v=0$. We get the

quantities at the wall as

$$h_{wall} = h_{i,2} + 0.5\frac{\Delta\eta}{\Delta\xi}\left(h_{i-1,2} - h_{i,2}\right)\cos\alpha \tag{3.23}$$

$$u_{wall} = u_{i,2} + 0.5\frac{\Delta\eta}{\Delta\xi}\left(u_{i-1,2} - u_{i,2}\right)\cos\alpha \tag{3.24}$$

For the side wall the condition $v = 0$ can not be applied . The velocity normal to the face should be zero , therefore on the side walls of the lateral channel the boundary conditions suggested by Bhallamudi(1992) are considered as

$$h_{ficticious} = h_{interior} \tag{3.25}$$

$$V_{ficticious} = V_{interior} \tag{3.26}$$

which means that the depth and magnitude of the resultant velocity at the ficticious points and the interior points are equal and the directions of the velocities are in such a way that it cancels the normal components . Finally we get the depth and velocities at the wall as:

$$V = \sqrt{u_{interior}^2 + v_{interior}^2} \tag{3.27}$$

$$u_{wall} = V\cos(\alpha - \theta)\cos\alpha \tag{3.28}$$

$$v_{wall} = V\cos(\alpha - \theta)\sin\alpha \tag{3.29}$$

3.4 Stability Condition

Courant-Friedrich-Levy condition has mathematical foundation for the linear equation. Shallow water equations are nonlinear and hence this condition can be used

as a guideline for the nonlinear equations but can not give full justification for such equation. Besides that it is not fully justified for TVD schemes . The condition for two dimensional flows is given as:

$$CN = \left(V + \sqrt{gh}\right) \Delta t \frac{\sqrt{\Delta\xi^2 + \Delta\eta^2}}{\Delta\xi\Delta\eta} \leq 1 \tag{3.30}$$

In terms of Δt

$$\Delta t = \frac{CN}{V + \sqrt{gh}} \frac{1}{\sqrt{\frac{1}{\Delta\xi^2} + \frac{1}{\Delta\eta^2}}} \tag{3.31}$$

where V is the velocity at the grid point and CN should be less than one. The scheme used in the present study is stable under some CFL conditions. In addition to CFL condition another factor γ is also important for the stability of this scheme. For stability γ should be such that

$$\gamma \geq \quad max|\lambda_{i,j}| \tag{3.32}$$

$$i = 1, i_{max}$$

$$j = 1, j_{max}$$

where $\lambda_{i,j}$ is the wave velocity at some node i, j

It appears that in some cases the value of γ may be relaxed and the behaviour of γ has been studied by Marinko Nujic (not yet published). The value of γ used in the present study is the value specified in Eqn(3.32).

Chapter 4

Varification of the Model

4.1 Introduction

The results of the mathematical model presented in the Chapter 2 and 3 are compared with the available laboratory test data (Hager , 1989). The numerical results are also compared with the approximate analytical solutions

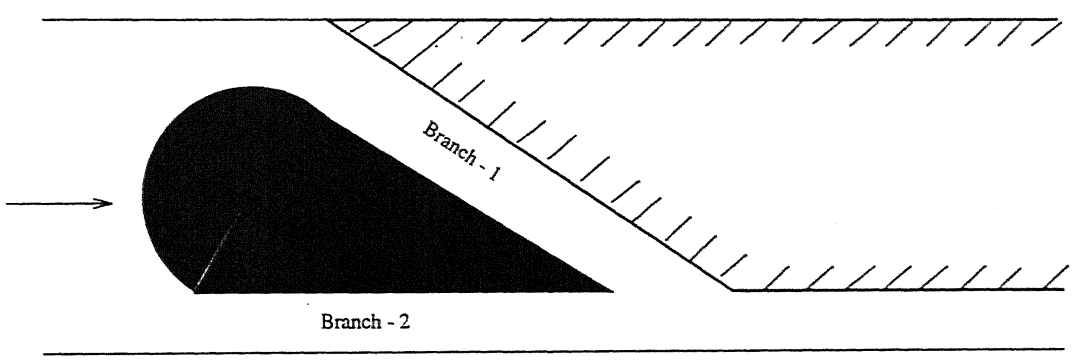

Fig(4.1): Plan View of Experimental Arrangement

of Hager. The experiments were conducted by Hager in a rectangular , horizontal channel of 50 cm width. Two confluence elements were inserted in the channel as shown in the Fig(4.1), making the width of the three branches equal to 99 mm each. Two junction angles $\alpha = 22.5^{\circ}$ and 45° were considered in this study. The flow depths were controlled by two vertical, movable gates which were placed immediately upstream of the junction . The length of the downstream branch was 60 cm and after this it again expanded to the full channel width of 50 cm. The main test section was situated between the gates and the end of the downstream branch. Two types of tests were conducted. In the first type, the flow depths h_u and h_l, the velocities V_u and V_l, the angles of the main wave front θ and the maximum flow depths h_{max} were measured in the majority of the runs. The Froude numbers covered the range $2.8 < F_r < 16$ for $\alpha = 22.5^{\circ}$ and $3.3 < F_r < 8.3$ for $\alpha = 45^{\circ}$. In the second type of tests the entire three-dimensional velocity field and the flow surfaces were recorded for three selected runs. These selected runs were made for $\alpha = 22.5^{\circ}$. A point gauge (± 0.1 mm) and a propeller velocity meter (± 3 cm/s) were used to take measurements of depths and velocity respectively. Details of the experiments are available in Ref (Hager, 1989).

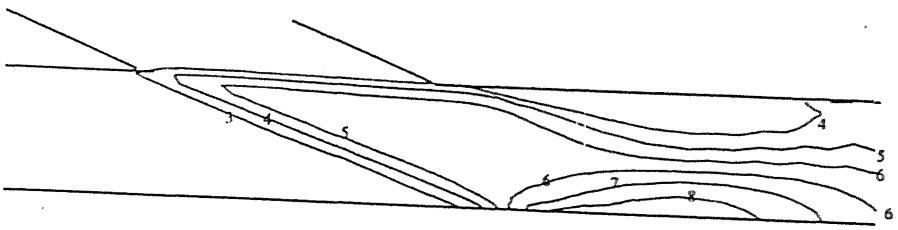

Fig(4.2)a: Water Surface Contours for Run 1 (Computed)

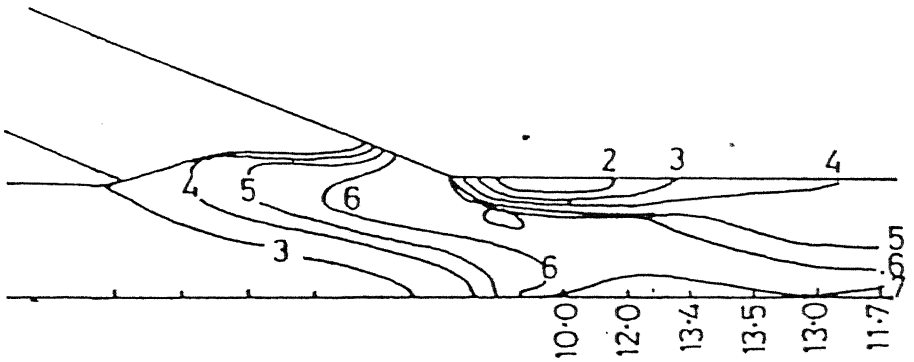

Fig(4.2)b: Water Surface Contours for Run 1 (Observed)

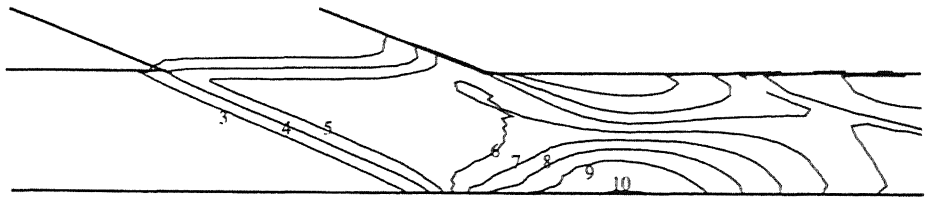

Fig(4.3)a: Water Surface Contours for Run 2 (Computed)

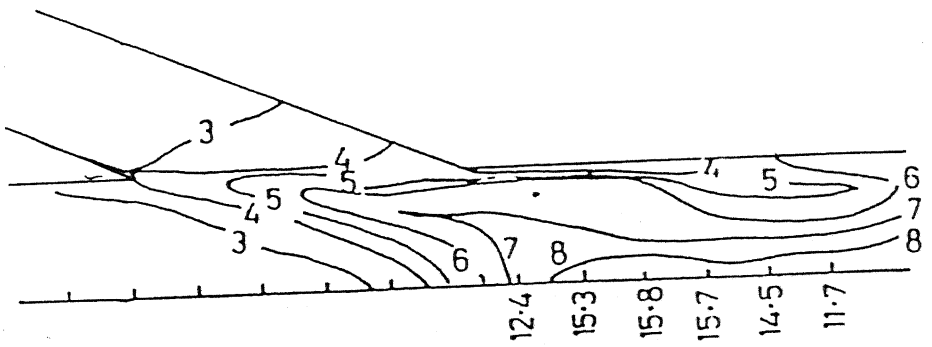

Fig(4.3)b: Water Surface Contours for Run 2 (Observed)

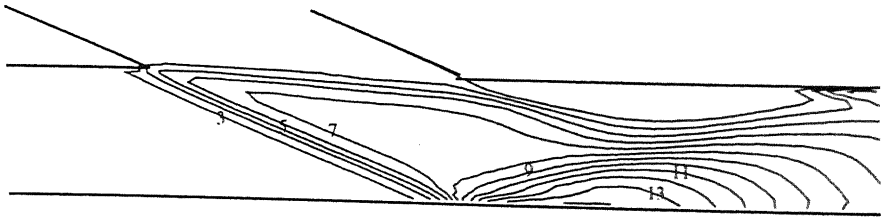

Fig(4.4)a: Water Surface Contours for Run 3 (Computed)

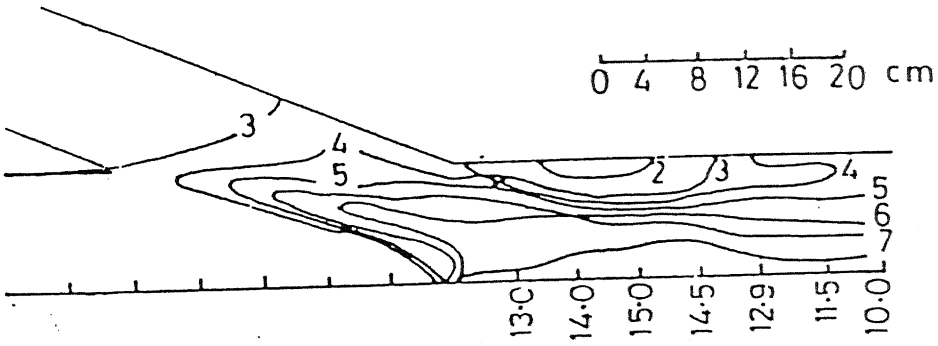

Fig(4.4)b: Water Surface Contours for Run 3 (Observed)

4.2 Study of Water Surface contours

The entire water surface profiles were measured by Hager for the following sets of inflow conditions

Run	F_U	F_L	$h_u(cm)$	$h_l(cm)$
1	5.25	6.2	2.65	1.98
2	4.5	4.5	2.65	2.65
3	6.2	5.25	2.65	3.58

Table 4.1 : Details of Hager's experiments of type 2

The numerical model presented in the previous chapter was run for the above test conditions using a numerical grid of $\Delta\xi = \Delta\eta = 1.724$ cm . This corresponds to 15 grids in the main channel. The computational step, Δt was controlled by the Courant number and grid size. The upper limit for the Courant Number to achieve numerical stability required some amount of numerical experimentation and a value of 0.6 was adopted for these runs. In addition to the Courant number there is another parameter γ in the Nujic's scheme which controls the spurious oscillations and hence stability. The value of γ for the above runs was taken to be equal to the maximum wave velocity . The roughness coefficient was assumed to be zero since no information on this was available in the literature. The computed water level contours for Runs 1,2 and 3 are shown in Fig(4.2a), Fig(4.3a) and Fig(4.4a) respectively. The measured water level contours are shown in Fig(4.2b), Fig(4.3b)

and Fig(4.4b) respectively. The comparison of computed and measured water level contours indicate that the nature of the water surface contour is simulated fairly well by the present numerical model. However the simulation of the water surface profile along the walls is not very good. This is reflected in the prediction of the maximum flow depth. This point is discussed in more detail in the next section. It has also been obsereved that the water surface contours are simulated much better if the depths in the two channels are of the same order. For example in Run 2 the depths in the main channel and the lateral channel are the same (2.65 cm) and the depth contours for this case are the best out of the three cases studied. It is thus concluded that the water surface contours are simulates qualitatively well by the numerical procedure of this study.

4.3 Prediction of Maximum Flow Depth

Tables 4.2 and 4.3 present the maximum flow depth predicted by the Hager's approximate method and the present numerical model, and also as measured in the experiments for different inflow conditions for $\alpha = 22.5°$ and $\alpha = 45°$ respectively. A comparison of numerical and analytical results for $\alpha = 22.5°$ is shown in Fig(4.5). It can be observed that agreement is good for some runs while it is not very satisfactory for some others. Both the numerical and analytical solutions are based upon shallow water flow assumptions. However, the approximate method assumes

a straight line shock front, line AC (in Fig(1.1)). However, the results from the numerical model, indicate that the main wavefront at the angle θ does not remain straight but becomes curved. This is also pointed out by Hager. From Tables 4.2 and 4.3 it can be noted that the results are better when $F_u h_u / F_l h_l$ is of the order of unity or the flows in the main channel is stronger than the flow in the lateral channel. Also the results are better for lower Froude number ($F_r < 7$) especially when the Froude number in the lateral channel is not very high.

Table 4.2: Table showing maximum depths computed numerically (h_n), analytically (h_a) and determined experimentally (h_e) (confluence angle = 22.5°)

h_u (cm.)	h_l (cm.)	F_u	F_l	h_n (cm.)	h_a (cm.)	h_e (cm.)
2.650	2.650	4.260	4.180	10.044	8.84	14.30
2.680	2.680	4.610	4.470	10.215	9.66	16.00
2.670	2.670	5.290	5.300	10.538	11.30	19.80
2.680	1.790	3.390	4.250	8.562	6.72	9.50
2.650	1.760	3.940	4.720	8.835	7.58	9.90
2.650	1.770	4.370	5.230	8.799	8.41	11.20
2.650	1.780	4.800	5.720	8.720	9.23	11.90
2.650	1.780	5.220	6.220	8.469	10.00	13.60
2.710	1.330	3.780	5.480	7.828	7.13	8.50
2.720	1.330	4.650	6.530	8.039	8.62	9.90
2.720	1.340	5.150	7.170	7.867	9.50	11.30
2.750	.640	3.420	7.180	3.390	6.47	8.50
2.740	.670	5.070	10.140	3.409	8.07	6.70
1.850	2.550	3.780	3.120	7.778	5.71	9.20
1.850	2.600	4.150	3.600	7.898	6.45	11.10
1.870	2.530	5.090	4.370	8.456	8.00	13.20
1.890	2.540	6.170	5.290	10.006	9.95	15.00
1.300	2.690	5.460	3.800	7.893	8.34	12.50
1.320	2.680	6.780	4.700	9.415	8.38	14.70
1.320	2.680	7.500	5.200	10.288	11.21	14.50
.620	2.700	6.280	2.800	5.786	3.40	8.80
.635	2.710	7.330	3.370	6.753	4.92	10.50
.645	2.680	9.220	4.520	8.533	6.68	15.40
.650	2.680	10.650	5.110	9.850	7.96	17.30
.350	2.540	13.110	4.690	7.412	6.08	17.70
.353	2.540	14.830	5.420	8.672	7.20	18.40
.320	1.310	10.550	5.100	4.811	3.87	6.60
.325	1.330	13.600	6.590	6.277	5.42	12.00
.340	1.380	15.600	7.640	7.656	6.76	14.80
.330	.660	11.220	7.860	3.831	3.77	5.50
.353	.710	14.940	10.500	5.730	5.77	10.00
.345	.345	8.640	8.640	2.212	2.49	2.90
.355	.345	15.110	15.110	4.089	4.86	8.10
.750	.370	6.050	8.760	2.322	3.13	3.80
.750	.373	9.140	13.070	3.555	4.79	6.20
.725	.725	4.760	4.760	2.690	2.72	3.70
.730	.730	7.180	7.180	3.860	4.27	5.60
.720	.720	9.670	9.670	5.195	5.90	10.20

Table 4.3: Table showing maximum depths computed numerically (h_n), analytically (h_a) and determined experimentally (h_e) (confluence angle = 45°)

h_u (cm.)	h_l (cm.)	F_u	F_l	h_n (cm.)	h_a (cm.)	h_e (cm.)
1.240	1.280	4.640	4.370	8.248	7.33	9.20
1.250	1.290	5.800	5.450	10.390	9.96	12.30
1.280	1.320	6.720	6.050	11.932	12.20	15.60
2.480	2.500	4.080	3.920	14.279	12.30	15.70
2.460	2.520	4.480	4.320	15.848	13.90	17.40
1.830	2.460	4.960	4.170	14.210	12.40	15.10
1.790	2.530	5.540	4.580	16.335	14.20	17.20
1.220	2.460	6.300	4.320	12.405	12.30	14.70
1.230	2.470	7.000	4.820	16.252	14.20	18.40
2.430	1.850	3.790	4.340	11.779	10.50	12.90
2.460	1.850	4.280	4.810	12.981	12.50	15.60
2.470	1.840	4.710	5.250	14.122	14.10	18.40
2.510	1.300	3.790	5.100	9.534	10.20	12.90
2.480	1.280	4.420	5.930	10.931	12.20	15.00
2.470	1.300	4.940	6.550	12.288	14.20	18.80
2.450	.680	3.300	6.580	6.180	7.70	8.60
2.480	.700	3.890	6.980	6.639	9.20	10.00
2.480	.690	4.560	8.300	7.546	11.11	13.20
.700	.750	5.530	5.160	5.684	5.30	7.70
.710	.760	8.110	7.400	8.493	8.89	13.00
.460	.500	5.410	4.740	3.534	3.32	4.50
.470	.510	6.700	6.120	4.647	4.59	6.20
.490	.530	7.070	6.530	5.147	5.16	7.60
.510	.560	7.150	6.530	5.449	5.46	8.50

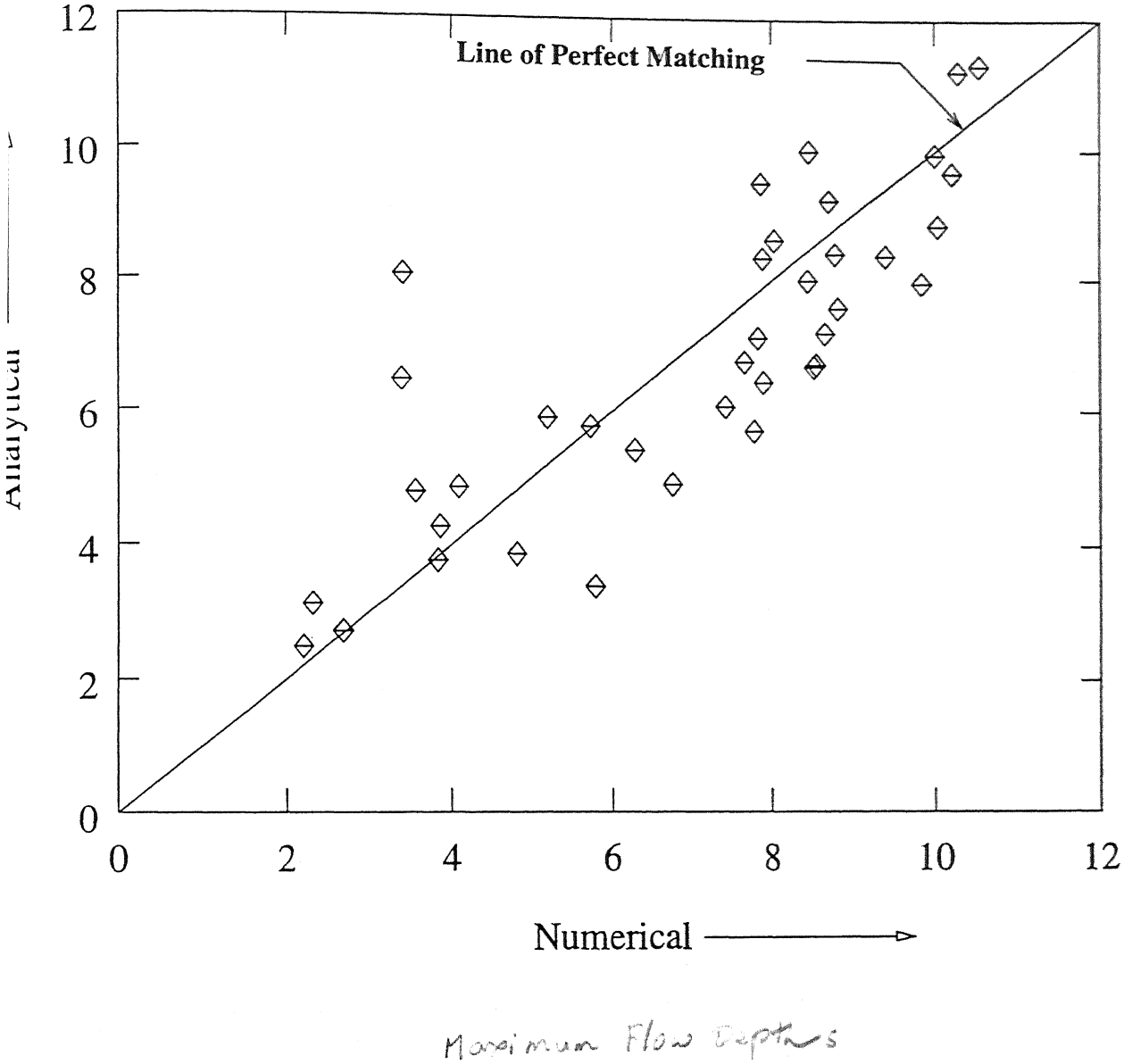

Maximum Flow Depths

Fig(4.5) Comparison of Numerical and Analytical Results for angle=22.5 ^{o}

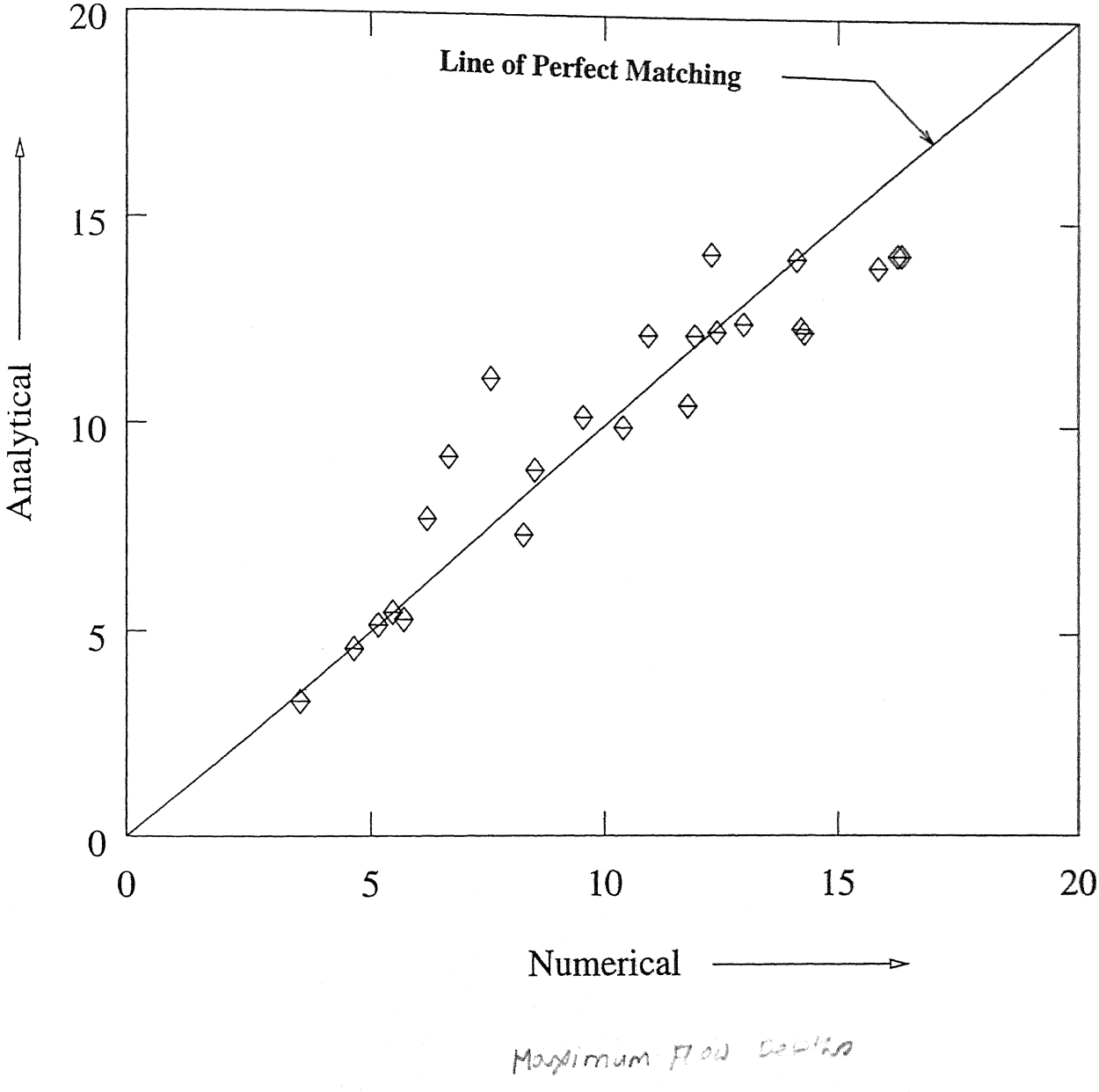

Maximum Flow Deviation

Fig(4.6) Comparison of Numerical and **Analytical Results for 45 °**

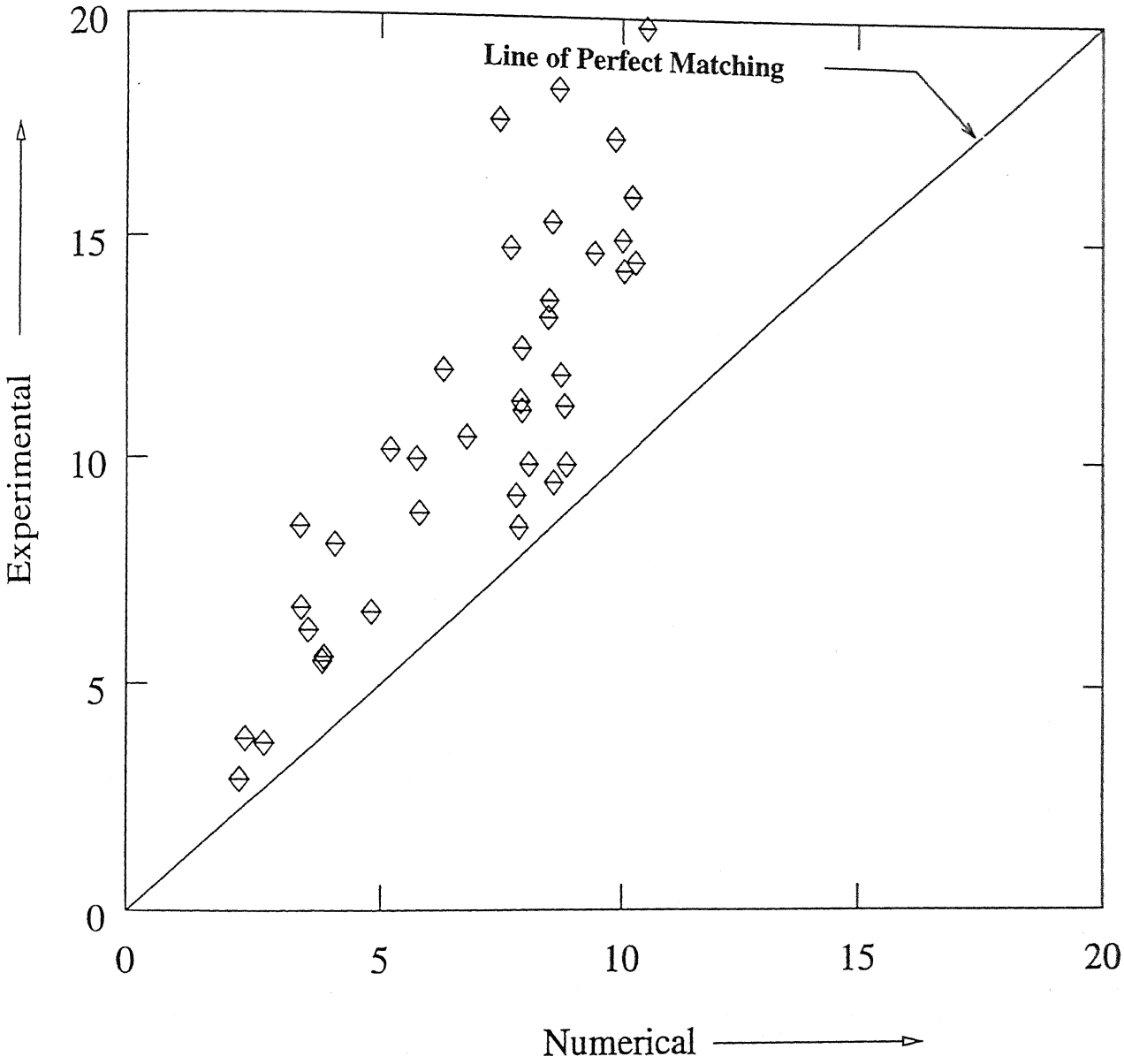

Fig (4.7) Comparison of Numerical and Experimental Results for angle=22.5°

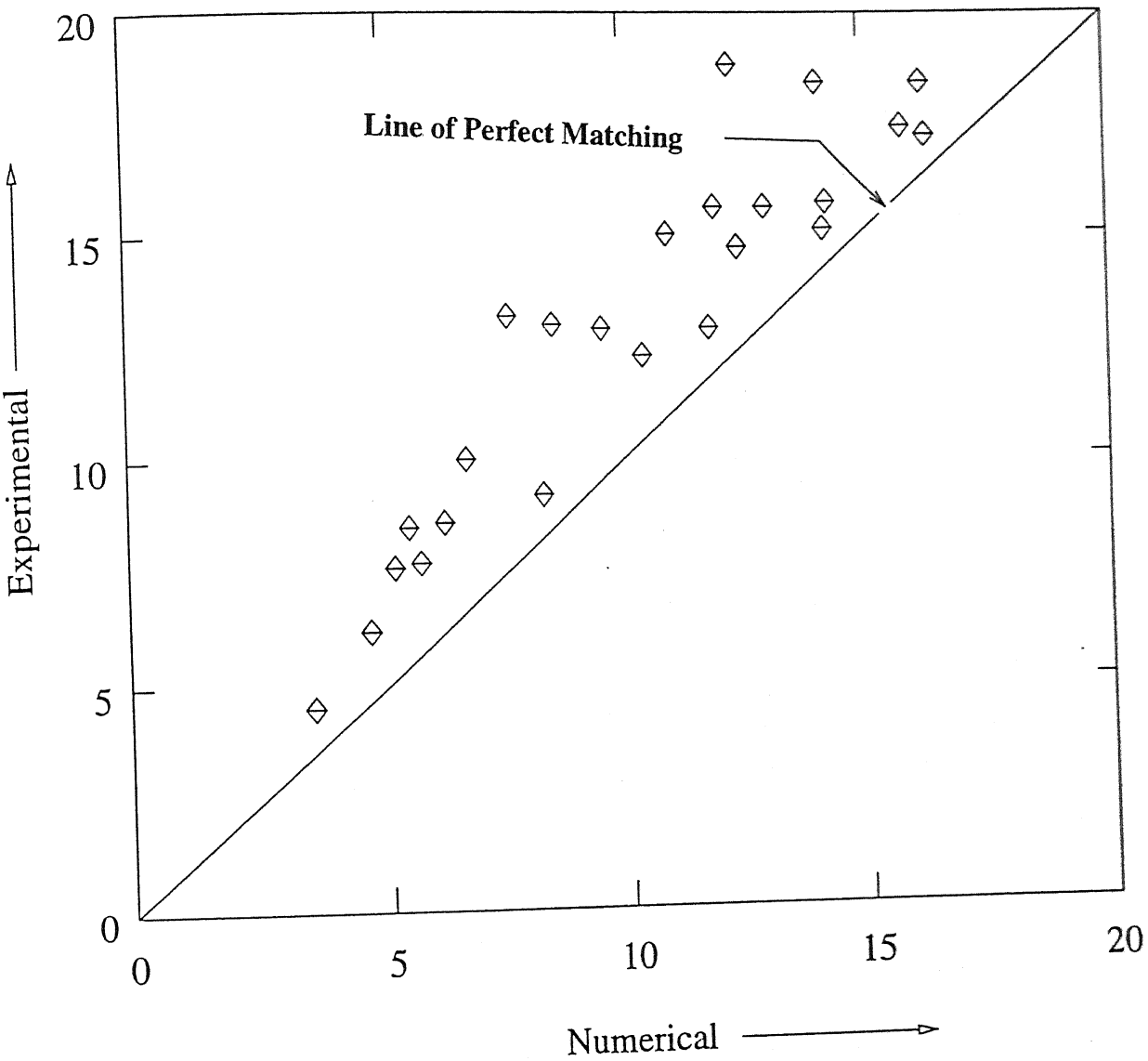

Fig(4.8) Comparison of Numerical and Experimental Results for angle=45^{o}

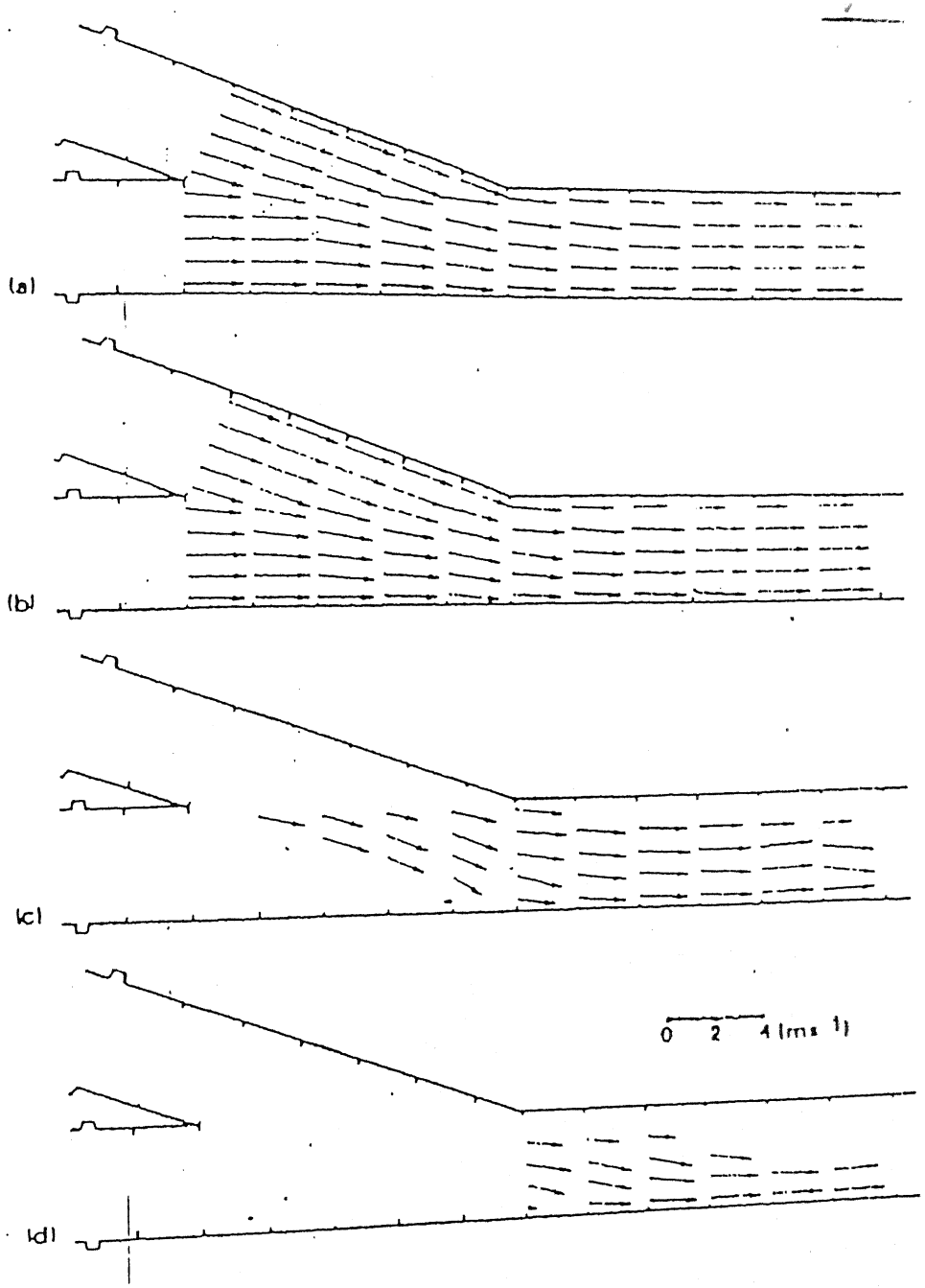

Fig(4.9): Velocity vectors at various elevations

Above Channel Bottom (a) 1.0 cm (b) 2.5 cm
(c) 5.0 cm (d) 7.5 cm

Fig(4.7) compares the numerical results with the experimental results for $\alpha = 22.5^o$. The matching of the numerical and experimental results is satisfactory only for the small values of maximum flow depth. But in the majority of cases the predicted maximum flow depth is underestimated by the numerical model . The error in the numerical prediction increases with the increase in the maximum flow depth. This indicates, as expected (Jimenez, 1987), that the shallow water assumptions breaks down when the flow depth in the channel is large compared to the channel width. The assumption of uniform velocity across the flow depth at a point may be another reason for the unsatisfactory performance of the numerical model. For example the three dimensional nature of the velocity field for Run 2 is shown in Fig(4.9). As can be seen, both the magnitude as well as the direction of velocity change across the depth.

The velocity vectors are seen to be parallel to the side walls in the two inflowing sections except near the confluence corner. Further in the junction, the flow near the outside walls remains parallel to the boundary, both at elevation $z = 1$ cm and $z = 2.5$ cm above the bottom. The streamlines turn to follow the main wave front at an angle θ. This turning is less near the bottom and becomes more pronounced towards the free surface. At $z = 5$ cm , the flow along the wave front turns toward the outer wall and impinges on it, creating stagnation conditions. A two dimensional model , whether numerical or analytical, can not simulate this effect completely.

This error due to the assumption of uniform velocity cross a vertical could also be significant in addition to the error due to the assumption of hydrostatic pressure distribution, (Sec. 2.2.1)

The comparison of the numerical and analytical results for $\alpha = 45^o$ is shown in Fig(4.6). It is clear that results of numerical study are better than the and the approximate method of Hager when the flow in the main channel is dominant (i.e. $F_u h_u / F_l h_l \geq 1$). This is especially so when the Froude number in the main channel is higher. While the numerical study predicts better than the Hager's method, still the maximum depth is underestimated in relation to the experimental results (Fig(4.7)). The Prediction of the maximum depth by the numerical method is much better when $\alpha = 45^o$ than for the case of 22.5^o. Thus it is concluded that the present numerical simulation gives better results than Hager's approximate method for predicting the maximum depth of flow in the junction with large confluence angle ($\alpha = 45^o$). However, for smaller confluence angle ($\alpha = 22.5^o$) the results of numerical simulation are of comparable accuracy with those of Hager's method.

4.4 Numerical Sensitivity of the Model

The present numerical model is sensitive to the parameters like Courant number (CN) and the coefficient γ. For the purpose of prediction of water surface contours CN = 0.6 gave satisfactory convergence. While testing the effect of CN value on the

convergence value of CN < 0.7 gave satisfactory results. The factor γ should be the maximum wave velocity for a time step. Hence the value of maximum wave velocity was used as the appropriate value for γin the present study. Though Nujic(1989) states that the above criteria for γ can be relaxed in some cases, In the absence of any criteria to decide the value, no relaxation was attempted. It is felt that the value of CN to be adopted in a study would depend upon the criteria adopted for the selection of γ. Numerical experimentations are needed in a specific problem to identify the best combination of CN and γ

Chapter 5

Summary and Conclusions

A two dimensional mathematical model is presented for analyzing the flow in a supercritical channel junction. An algebraic coordinate transformations is used to obtain a boundary fitted orthogonal computational grid. This makes it easier to apply the side wall boundary conditions. The unsteady governing equations are used in a false transient approach to simulate the steady supercritical flow.

The salient conclusions of present study are as follows.

1. Regarding the maximum depth of the confluence the numerical prediction is nearer to the experimental results when

   (a) the flow in the main channel is dominant ($F_u h_u / F_l h_l \geq 1$ and especially when $F_u \geq F_l$)

   (b) the depths in the main channel and the branch channel are of the same order of magnitude

   (c) the depth to width ratio is small and

(d) the confluence angle is large

2. Regarding the Water Surface Contours the numerical prediction of the water surface contours at the junction agree adequately with the experimental observation qualitatively. However, exact quantitative predictions at the boundaries can not be achieved due to the inherent nature of modelling.

3. The present numerical simulation gives better results than Hager's approximate method for predicting the maximum depth of flow in the junction with large confluence angle ($\alpha \approx 45°$). However, for smaller confluence angle ($\alpha \approx 22.5°$) the results of numerical simulation are of comparable accuracy with those of Hager's method.

REFERENCES

Abbott, M.B., (1975), "Weak Solutions of the Equations of Open Channel Flow ", in *Unsteady Flow in Open Channels* , Mahmood,K. and Yevjevich, V. (eds.). Water Resources Publications, Chapter 7, pp. 283-311.

Abbott, M.B., (1979), *Computational Hydraulics; Elements of the Theory of Free Surface Flow* , Pitman Publishing Limited, London.

Anderson, D.A., Tannehill, J.D. and Pletcher, R.H., (1984), *Computational Fluid Mechanics and Heat transfer*, McGraw-Hill,New York.

Bhallamudi, S.M. and Chaudhary, M.H., (1992), "Computation of flows in Open-Channel Transitions", Journal of Hydraulic Research, IAHR, Vol. 30, No.1, pp. 77-93.

Bhargava, R., (1991), "Computation of Supercritical Flow in Channel Junctions", thesis submitted for the degree of Master of Technology, Indian Institute of Technology, Kanpur.

Behlke, C.E. and Pritchett, H.D., (1966), "The design of Supercritical Channel Junctions", Highway Res. Record, No. 123, Publication 1365, 17-35, Highway Reasearch Board, National Research Council, Washington, D.C.

Bowers, C.E., (1950), "Studies of Open Channel Junctions", Technical Paper No. 6, Series B, Part v, Hydraulic Model Studies for Whiting Field Naval Air Station, University of Minnesota, St. Anthony Falls Hydraulic Laboratory.

Cunge, J.A., (1975), "Rapidly Varying Flow in Power and Pumping Canals, in Unsteady Flow in Open Channels", (Eds. Mahmood, K. and Yevjevich, V.), Water Resources Publications, Fort Collins.

Chaudhary, M.H. (1993), *Open-Channel Flow*, Prentice hall, New Jersey.

Dakshinamoorthy, S.,(1973), "Some Numerical Studies on Supercritical Flow Problems", thesis submitted for the degree of Doctor of Philosophy, Indian Institute of Technology, Kanpur.

Dakshinamoorthy, S.,(1977), "High Velocity Flow through Expansions ",17^{th} Congress IAHR, Baden-Baden, Vol. 2, pp.373-381.

Gerodetti, M. ,(1978), "Schussrinnen im Strassenbau", Strasse und Verkehr, Zurich, 64(7), pp. 271-275. (in German).

Greated, C.A. ,(1968), "Supercritical Flow ThroughJunctions", La Houille Blanche, 23(8), pp. 693-695.

Hager, W.H. ,(1989), "Supercritical Flow in Channel Junctions", Journal of Hydr. Eng., ASCE, Vol. 115, No. 5, pp. 595-616.

Herbich, J. B. and Walsh, P., (1972), "Supercritical Flow in Rectangular Expansions," Jour. Hydr. Div., Amer. Soc. Civ. Engrs., Vol. 98, No. 9, Sept., pp.1691-1700.

Ippen, A.T. and Dawson, J.H., (1951), "Design of Channel Contractions", Symposium on High-Velocity Flow in Open Channels, Trans. Amer. Soc. Civ. Engrs., Vol. 116, pp. 326-346.

Ippen, A. T. and Harlman, D. R. F. , (1950), *Studies on the Validity of the Hydraulic Analogy to Supersonic Flow* Parts I and II, USAF Technical Report No. 5985, May.

Nujic, Marinko, (1995), "Efficient implementation of non oscillatory schemes for computation of free-surface flow",Journal of Hydraulic Research, Vol. 33, No. 1 pp. 101-111.

Jimenez, O.F., (1987), "Computation of Supercritical Flow in Open Channels", thesis submitted for the degree of Master of Science, Washington state University, Pullman.

Jimenez, O.F. and Chaudhary, M.H., (1988), "Computation of Supercritical Free-Surface flows", Jour. of Hydr. Eng., ASCE, Vol. 114, No. 4, pp. 377-395.

Liggett, J.A. and Vasudev, S.U., (1965), "Slope and Friction Effects in Two-dimensional High Speed Flow", 11^{th} Int. Congress, IAHR, Leningrad, Vol. 1, Paper 1.25.

Pandolfi, M., (1972), "Numerical Experiments on Free Surface Water Motion with Bores", 4th Int. Conference on Numerical Methods in Fluid Dynamics, Lecture Notes in Physic, Springer-Verlag, pp. 304-312.

Puri, A. N. and Kuo, C. Y. (1985), "Numerical Modelling of Subcritical Open Channel Flow Using The k-ϵ Turbulence Model and The Penalty Function Finite Element Technique," Appl. Math. Modelling, vol. 9, No. 2, Apr., pp.82-88.

Rastogi, A. K. and Rodi, W., (1978), "Predictions of Heat and Mass transfer in Open Channels ," Jour. Hydr. Engr., Amer. Soc. Civ. engrs., vol. 104, no. 3, March, pp.397-419

Roache, P.J., (1972), *Computational Fluid Dynamics*, Hermosa Publishers.

Schnitter, G., Muller, R. Caprez, V. and Bisaz, E., (1955), "Modellversuche

fuer Kraftwerkbauten im Wallis", ausgefuehrt an der Hydraulischen Abteilung der Versuchsanstalt fuer Wassebau und Erdbau an der ETH, Wasser-und Energie-wirtschaft. 47(5-7). (in German).

Stokes, J.J.,(1957), *Water waves*, Interscience Publishers, New York.

Subramanya, K. (1995), *Flow in Open Channels*, Tata McGraw-Hill, New Delhi.

Villagas, F., (1966), " Design of the Punchina Spillway", Water Power and Dam Construction, Nov., pp. 32-34

Vreugdenhil, C.B, and Wijbenga, J.H.A,(1982) "Computations of Flow Patterns in Rivers," Jour. Hydr. Div., Amer. Soc. Civ.Engrs., Vol. 108. No.11, pp. 1296-1310.